Acta Cryst. (1963). **16**, 174

Fourier Projections of Unpaired Electron Densities*

By S. J. Pickart

U.S. Naval Ordnance Laboratory, Silver Spring, Maryland; Brookhaven National Laboratory, Upton, New York, U.S.A.

(*Received* 13 *February* 1962 *and in revised form* 16 *April* 1962)

The determination of outer *d*-electron configurations from magnetic scattering amplitudes by Fourier synthesis is discussed, particularly with reference to diffraction effects, which are investigated by varying the number of coefficients used in the syntheses. It is concluded that reliable information may be gained by this method about the symmetry of the unpaired electron distribution.

Introduction

Fourier syntheses using neutron magnetic scattering data from iron series metals and compounds have been performed recently to illustrate the anisotropy of the unpaired electron distribution. (Pickart & Nathans, 1961; Alperin, 1961; Shull & Yamada, 1961). Since this information is relevant to theories concerning the electronic structure of the metallic atoms in these materials, it is necessary to ask how reliably it can be extracted from the scattering data by this method. The purpose of this note is to examine the symmetry features of two-dimensional projections of typical spin densities, and to investigate their sensitivity to diffraction effects by varying the number of coefficients used in the syntheses.

As a preliminary it may be useful to recall some of the differences between X-ray scattering factors and neutron magnetic form factors that are likely to influence the inversion process. First and most important is the fact that the unpaired electrons giving rise to the iron group atom's net moment are in 3*d* shells. Since their mean radius is much larger than that of the total electronic charge, the magnetic form factor falls off more rapidly with angle than the X-ray scattering factor, and diffraction fringes caused by omitting reflections at angles higher than the observable limit are less troublesome. Another consequence is the sensitivity of the measurements to the valence electron configuration, which, although representing a small perturbation of the spherical symmetry of the total electron cloud, is singled out by the neutron magnetic scattering process. Secondly, at least as far as polarized neutron measurements are concerned, the magnetic amplitude is determined relative to the nuclear in phase as well as magnitude (Nathans, 1960). This fact, though limiting the present application of such measurements to known structures, eliminates the ambiguity in sign of the coefficients in the synthesis. Finally, temperature motions which tend to blur the electron density are also corrected for by virtue of the above fact, provided the vibration amplitude is the same for the magnetic electrons and the nuclei. All of these considerations would suggest that details of the outer electron configuration determined from magnetic form factors, in particular any departures from spherical symmetry, are more reliable than determinations using X-ray scattering factors, about which there has been some controversy (Carpenter, 1960; Ibers, 1960; Hovi & Pautamo, 1960).

In what follows the theoretical anisotropic form factors for Fe calculated by Weiss & Freeman (1959) were used to investigate the inversion process, since this procedure frees the interpretation from uncertainties inherent in experimental data. Following these considerations is a discussion of what effect the resolution function and experimental errors have on some actual density maps obtained by syntheses using measured magnetic scattering amplitudes. It should be emphasized that what one actually obtains is a picture of the *magnetic moment* distribution, which may be interpreted in terms of the unpaired *electron* distribution only if the orbital moment is quenched. This is very nearly so in all the cases thus far treated.

Projections using theoretical anisotropic form factors

Weiss & Freeman (1959) calculated anisotropic scattering factors for electrons in the e_g and t_{2g} symmetry orbitals of the normally degenerate 3*d*-level in Fe. In order to get a better idea of what to expect from actual projections that use observed data, projections were prepared using these calculated scattering factors in the bcc cell as a function of the cut-off point. The cut-offs are shown in Fig. 1 with relation to Weiss & Freeman's isotropic scattering factor.

In order to investigate the amount of charge recovered as a function of the cut-off point, an (001) projection was prepared from the calculated spherical form factor by summing (*hk*0) reflections, since the atoms are almost completely resolved in this projec-

* Work performed under the auspices of the U.S. Atomic Energy Commission.

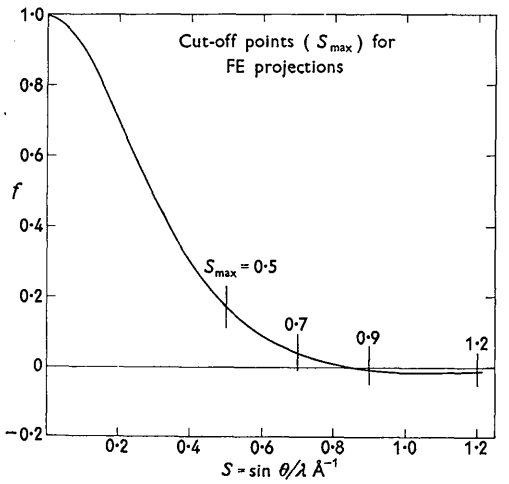

Fig. 1. Weiss & Freeman's (1959) spherical form factor for the 3*d* electrons in Fe, showing the cut-offs used in preparing the present syntheses.

tion. The resulting two-dimensional charge density function was integrated out to a radius equal to half the projected nearest neighbor distance, with the results shown in Table 1 (S_{max} = cut-off in $\sin\theta/\lambda$, N = number of terms used in the Fourier series). From this it can be seen that not much will be gained in the electron count by going to higher angles.

Table 1. *Integration of* Fe(001) *projections*

S_{max}	N	% Total charge
0·5 Å^{-1}	12	96·6
0·7	24	97·9
0·9	44	98·7
1·2	68	98·5

In Fig. 2 are shown projections of the e_g density on (110) as a function of cut-off point, prepared by summing (*hhl*) reflections. One-eighth of the plane is shown, with a corner atom at the upper left and a projected body-centered atom at the lower left. Deformation of the charge into the lobes along the cube edges is clearly visible for S_{max} = 0·9 Å^{-1}. Along the face diagonal one sees a peak of higher density, resulting from the superposition of two foreshortened lobes.

We repeated this same synthesis using $F_{anisotropic} - F_{spherical}$ as coefficients, *i.e.*, subtracting an isotropic charge density with equivalent radial dependence. This procedure will help both in cancelling diffraction fringes from the two projections, if they are similar, and in removing apparent anisotropies generated by the overlapping of spherical densities. As seen from Fig. 3, the characteristic pattern is identifiable at a lower cut-off, S_{max} = 0·7 Å^{-1}.

For the sake of completeness, Fig. 4 represents dif-

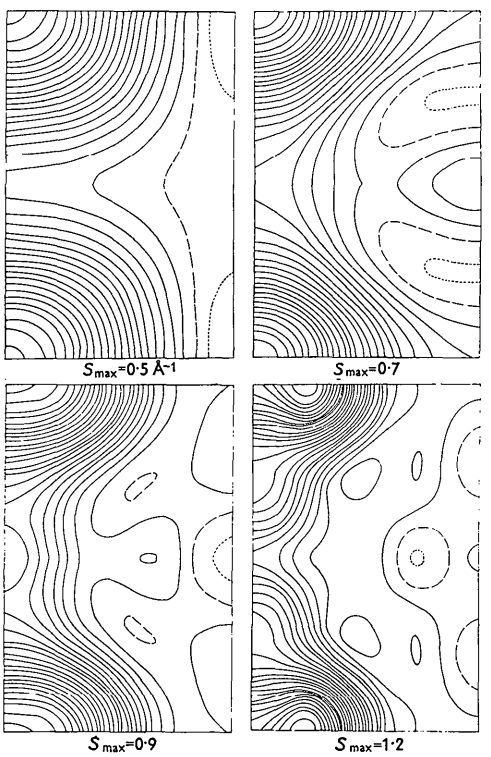

Fig. 2. Fourier syntheses of e_g electron density on the (110) plane of bcc Fe as a function of cut-off point. Solid lines correspond to positive density, dashed to zero, and dotted to negative. (This convention will be used in all the following figures). Contours are at intervals of 0·152 μ_B/Å^2.

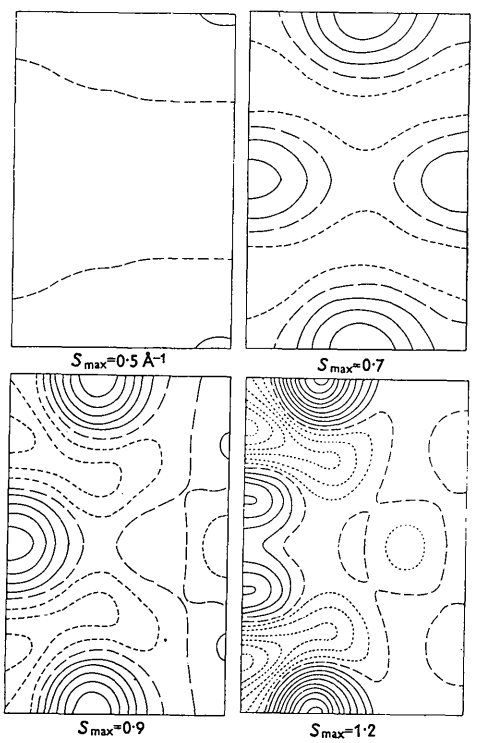

Fig. 3. (110) Difference syntheses in bcc Fe as a function of cut-off point. Nomenclature as in Fig. 2.

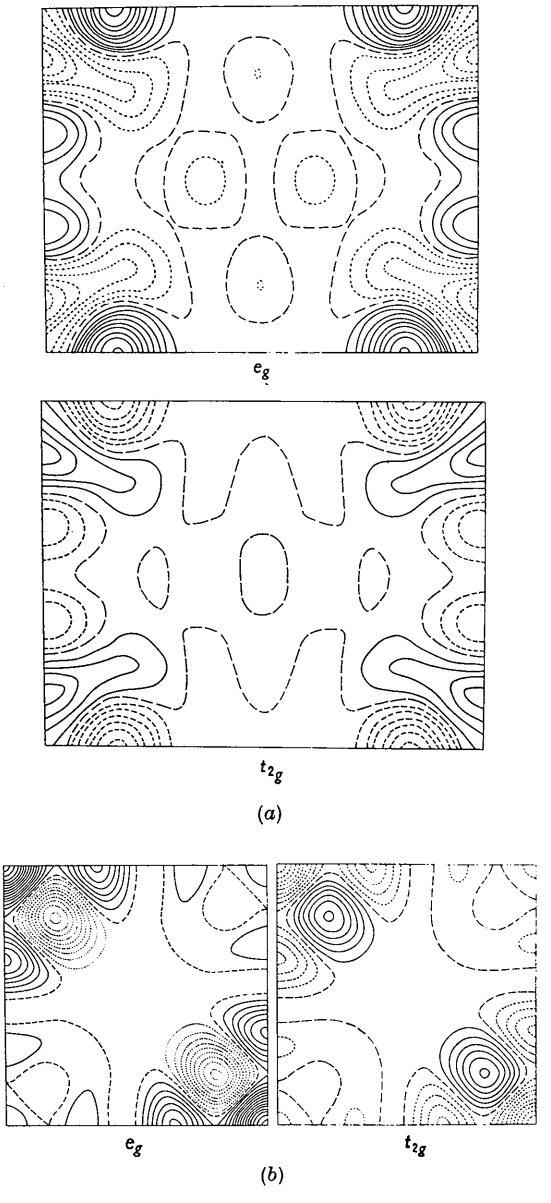

Fig. 4. (*a*) Difference projection of e_g and t_{2g} charge densities on (110), contour intervals at 0·152 $\mu_B/\text{Å}^2$. (*b*) Same as 4(*a*) but projected on (001), contour intervals at 0·107 $\mu_B/\text{Å}^2$.

ference projections on the (110) and (001) planes for charge distributions of both e_g and t_{2g} symmetry, carried out to $S_{max}=1{\cdot}2$ Å^{-1}. One-quarter of the plane is shown in these cases.

Projections using measured polarized neutron data

Measurement of magnetic structure factors using polarized neutrons has been amply described elsewhere (Nathans, Shull, Shirane & Andresen, 1959; Nathans, 1960). The interest here is in pointing out the influence of the resolution function and the standard error of the observations on the previously synthesized spin density distributions in ordered Fe_3Al (Pickart & Nathans, 1961). A difference projection ($F_{observed}-F_{spherical}$) on (110) using data collected out to $S_{max}=0{\cdot}9$ Å^{-1} is shown in Fig. 5(*a*). This projection, which covers one-sixteenth the total area of the (110) plane, indicates predominantly e_g symmetry for the Fe(I) atom (which has only Fe near neighbors) and essentially spherical symmetry for the Fe(II) atoms (half Fe and half Al near neighbors). There is no magnetic moment residing on the Al atoms.

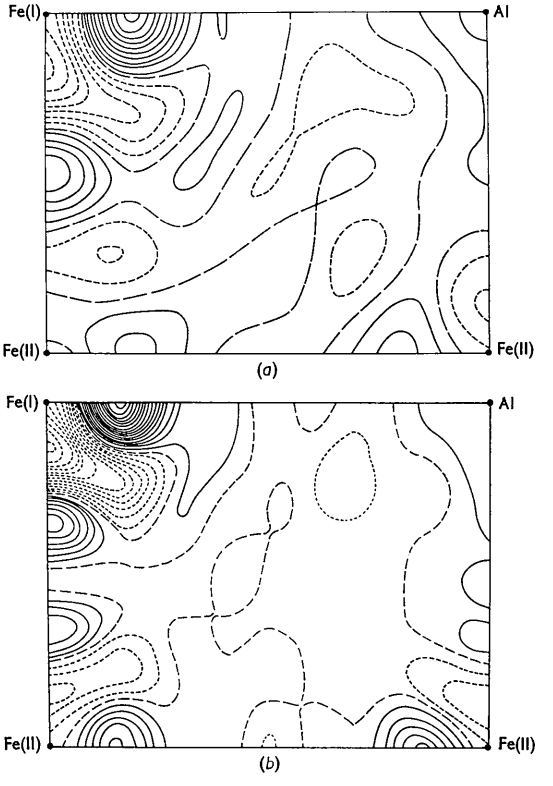

Fig. 5. (*a*) Difference projection $F_{obs.}-F_{spherical}$ (calculated) on the (110) plane of Fe_3Al. ($S_{max}=0{\cdot}9$ Å^{-1}). Contours at intervals of 0·063 $\mu_B/\text{Å}^2$. (*b*) Same section, showing effect of extrapolating data to 1·2 Å^{-1}.

In the resolution function derived by James (1954), the synthesized image of a point scatterer in a crystal has a radius $r=0{\cdot}61d$, where d is the smallest spacing used in the synthesis. This becomes

$$r=0{\cdot}61/(2S_{max})=0{\cdot}35 \text{ Å}$$

for the projection in 5(*a*). This is of the order of the width of the observed lobes, since the section shown measures 1·44 × 2·04 Å. The effect of decreasing the first zero of the resolution function to 0·25 Å, by supplying calculated data out to 1·2 Å^{-1}, is shown in Fig. 5(*b*). Besides sharpening up the detail around the Fe(I) atom, a slight preference of the Fe(II) atoms for

e_g symmetry over the two-to-three spherical admixture becomes apparent. This latter conclusion had been drawn from trial and error analysis of the experimental data; its confirmation in the projection 5(*b*) is purely a result of extrapolating the data, and here serves only as an example of the type of detail that could become recognizable if more data were available.

The error in the density for two-dimensional centrosymmetric projections depends differently on the standard error of the structure factors depending on whether $\sigma(F)$ is proportional to F or independent of it, though the difference does not amount to much in practical cases (Lipson & Cochran, 1953). $\sigma(F)$ fluctuated somewhat in the polarized beam data mentioned here but for the present purposes it may be considered constant. For this case, Lipson & Cochran (1953) give

$$\sigma(\varrho)=[\pi S^2_{\max}/A_c]^{\frac{1}{2}}\sigma(F)$$

where A_c is the area of the projected plane. If $\sigma(F)$ is taken to be constant at one per cent of the strongest structure factor, an overgenerous estimate, we find that $\sigma(\varrho)=0{\cdot}034\mu_B/\text{Å}^2$, which is approximately one-half the spacing of the contours in 5(*a*).

Conclusion

It may be concluded that, although termination and observational errors are not completely removed from current projections of unpaired electron densities, over-all features are nevertheless recognizable in sufficient detail to give reliable information about the symmetry of the unpaired electron distribution. Improvement can of course be made by collecting three-dimensional data, as Shull & Yamada (1961) have done for Fe, though this will be more advantageous in cases where the structure is of enough complexity that superposition in the projection is a real problem. In cases such as discussed here, the obvious next step would be to extend the measurements to higher scattering angles so as to improve the resolution.

During this work the author had numerous and valuable discussions with Dr R. Nathans and Dr H. A. Alperin. Thanks are also due to Dr B. C. Frazer for commenting on the manuscript.

References

ALPERIN, H. A. (1961). International Conference on Magnetism and Crystallography, Kyoto, Japan.
CARPENTER, G. B. (1960). *J. Chem. Phys.* **32**, 525.
HOVI, V. & PAUTAMO, Y. (1960). *Ann. Acad. Sci. Fenn. A VI*, no. 53.
IBERS, J. A. (1960). *J. Chem. Phys.* **33**, 299.
JAMES, R. W. (1954). *The Optical Principles of the Diffraction of X-rays*, p. 400. London: Bell.
LIPSON, H. & COCHRAN, W. (1953). *The Determination of Crystal Structures*, p. 288. London: Bell.
NATHANS, R. (1960). *J. Appl. Phys.* **31**, 350 S.
NATHANS, R., SHULL, C. G., SHIRANE, G. & ANDRESEN, A. (1959). *J. Phys. Chem. Solids*, **10**, 138.
PICKART, S. J. & NATHANS, R. (1961). *Phys. Rev.* **123**, 1163.
SHULL, C. G. & YAMADA, Y. (1961). International Conference on Magnetism and Crystallography, Kyoto, Japan.
WEISS, R. J. & FREEMAN, A. J. (1959). *J. Phys. Chem. Solids*, **10**, 147.

Acta Cryst. (1963). **16**, 177

The Structure of Aluminum Tetroxycarbide

BY G. A. JEFFREY AND M. SLAUGHTER*
The Crystallography Laboratory, The University of Pittsburgh, Pittsburgh 13, *Pa., U.S.A.*

(*Received* 29 *March* 1962)

Aluminum tetroxycarbide, Al_4O_4C, is a high temperature reaction product in the aluminum oxide carbide system. Its structure has been determined by single crystal analysis of three-dimensional Cu $K\alpha$ data. The structure was solved from the Patterson synthesis, and refined by differential Fourier synthesis methods.

The structure is based on $Al(O_3C)$ tetrahedra which share corners and edges. The unusual feature of the structure is a chain of tetrahedra which are linked alternately by sharing edges and corners. The observed Al–O bond lengths range from 1·71 to 1·87 Å, the Al–C from 1·91 to 1·98 Å, with standard deviations of 0·01 Å. There are two short non-bonded distances associated with the shared edge of the tetrahedra, Al · · · Al 2·63 Å, and O · · · O 2·53 Å.

Introduction

Aluminum tetroxycarbide, Al_4O_4C, was first recognized by Foster, Long & Hunter (1956) as a chemically distinct phase formed by high temperature reaction at about 1800 °C. in the aluminum oxide and carbide system. The other phases identified were δ-Al_2O_3, Al_2CO and Al_4C_3. The conditions for the formation of δ-Al_2O_3 by high temperature reactions have been dis-

* Present address, Dept. of Geology, University of Missouri.